THE JOURNAL OF BIOLOGICAL CHEMISTRY VOL. 286, NO. 34, pp. 30097–30106, August 26, 2011

Aurora-A Phosphorylates Augmin Complex Component Hice1 Protein at an N-terminal Serine/Threonine Cluster to Modulate Its Microtubule Binding Activity during Spindle Assembly*

Received for publication, May 31, 2011, and in revised form, June 23, 2011 Published, JBC Papers in Press, June 24, 2011, DOI 10.1074/jbc.M111.266767

Connie Y. Tsai[‡1], Bryan Ngo[‡], Anjali Tapadia[‡], Pang-Hung Hsu[§], Guikai Wu[‡2], and Wen-Hwa Lee[‡3,4]

From the [‡]Department of Biological Chemistry, University of California, Irvine, California 92697 and the [§]Department of Life Science and Institute of Bioscience and Biotechnology, National Taiwan Ocean University, Keelung 20224, Taiwan

Proper assembly of mitotic spindles requires Hice1, a spindle-associated protein. Hice1 possesses direct microtubule binding activity at its N-terminal region and contributes to intraspindle microtubule nucleation as a subunit of the Augmin complex. However, whether microtubule binding activity of Hice1 is modulated by mitotic regulators remains unexplored. Here, we found that Aurora-A kinase, a major mitotic kinase, specifically binds to and phosphorylates Hice1. We identified four serine/threonine clusters on Hice1 that can be phosphorylated by Aurora-A *in vitro*. Of the four clusters, the Ser/Thr-17–21 cluster was the most critical for bipolar spindle assembly, whereas other phospho-deficient point mutants had a minimal effect on spindle assembly. Immunostaining with a phospho-Ser-19/20 phospho-specific antibody revealed that phosphorylated Hice1 primarily localizes to spindle poles during prophase to metaphase but gradually diminishes after anaphase. Consistently, the phospho-mimic 17–21E mutant reduced microtubule binding activity *in vitro* and diminished localization to spindles *in vivo*. Furthermore, expression of the 17–21E mutant led to decreased association of Fam29a, an Augmin component, with spindles. On the other hand, expression of the phospho-deficient 17–21A mutant permitted intraspindle nucleation but delayed the separation of early mitotic spindle poles and the timely mitotic progression. Taken together, these results suggest that Aurora-A modulates the microtubule binding activity of Hice1 in a spatiotemporal manner for proper bipolar spindle assembly.

In eukaryotic cells, proper assembly of a dynamic bipolar spindle is vital for efficient chromosome congression and subsequent accurate segregation into two progeny cells (1–3). Deregulation of spindle assembly factors often leads to segregation errors. Spindle assembly requires *de novo* microtubule nucleation that is mediated by the classical centrosome-dependent pathway and two centrosome-independent pathways (3–6). Centrosome-independent microtubule nucleation can be mediated by the Ran-GTP pathway in a chromatin-dependent manner (7–11) or by the Augmin complex (also called homologous to Augmin subunits (HAUS)) from within the spindle. Altogether, these nucleation pathways contribute to proper assembly of bipolar spindles and allow faithful and efficient chromosome alignment and segregation.

The Augmin complex is an evolutionarily conserved eight-subunit protein complex (12–19). This complex associates with the γ-tubulin ring complex to facilitate microtubule nucleation on the basis of preexisting microtubules inside the spindle, thereby promoting the formation of dynamically stable bipolar spindles (12–16). Each subunit of this complex has been functionally validated to be important for microtubule nucleation from within the spindle and, thus, to be critical for proper spindle assembly (13–18).

We have previously shown that Hice1,[5] a critical Augmin component, contributes to spindle integrity and faithful mitotic division (20). Structurally, the Hice1 protein harbors a highly basic microtubule binding domain (amino acids 1–149) that has a direct microtubule binding activity and two coiled-coil domains (amino acids 150–228 and 263–329) that are important for protein-protein interactions (20, 21). Depletion of Hice1 causes mitotic delay, aberrant spindle configurations, chromosome misalignment, and erroneous cytokinesis, in part because of defective microtubule nucleation (13–21). Hice1 is distinct from other Augmin subunits in that its N-terminal region is enriched with basic and serine/threonine residues that enable its direct binding to microtubules. The microtubule binding activity, presumably mediated by electrostatic affinity between basic residues of Hice1 and acidic residues of β-tubulin, is critical for Hice1 to bind to and stabilize microtubules *in vitro* and *in vivo* and could be important for the function and regulation of the Augmin complex as a whole.

* This work was supported, in whole or in part, by National Institutes of Health Grant CA107568 (to W.-H. L.).

[1] Supported by a Department of Defense Congressionally Directed Medical Research Program Predoctoral Fellowship.

[2] To whom correspondence should be addressed: Dept. of Biological Chemistry, School of Medicine, University of California Irvine, 124 Sprague Hall, Irvine, CA 92697-4037. Tel.: 949-824-4492; Fax: 949-824-9767; E-mail: gwu@uci.edu.

[3] To whom correspondence should be addressed: Dept. of Biological Chemistry, School of Medicine, University of California Irvine, 124 Sprague Hall, Irvine, CA 92697-4037. Tel.: 949-824-4492; Fax: 949-824-9767; E-mail: whlee@uci.edu.

[4] Serves as a member of the board of directors of GeneTex, Inc. This arrangement has been reviewed and approved by the Conflict of Interest committee of the University of California Irvine.

[5] The abbreviations used are: Hice1, Hec1-interacting and centrosome-associated 1; PIPES, 1,4-piperazinediethanesulfonic acid; λ-PPase, lambda protein phosphatase.

Despite this understanding of Hice1, whether mitotic regulators modulate its microtubule binding activity remains unexplored. Regulatory mitotic kinases are known to directly phosphorylate various microtubule-associated proteins to regulate almost every aspect of mitosis. Aurora-A kinase is a prominent regulator of several mitotic processes, including centrosome maturation, mitotic entry, and spindle assembly (22, 23). Studies using a wide variety of model organisms revealed that perturbation of Aurora-A function leads to a multitude of mitotic defects, such as the formation of monopolar spindles and unstable bipolar spindles (24–28).

In this study, we investigated whether the microtubule binding activity of Hice1 can be regulated by Aurora-A via direct phosphorylation. We further explored whether the phosphorylation of Hice1 by Aurora-A facilitates intraspindle microtubule nucleation during bipolar spindle assembly to ensure accurate chromosome segregation in human cells.

EXPERIMENTAL PROCEDURES

Cloning—Site-directed mutagenesis was performed on the pEGFP-N1-Hice1 construct to create desired mutations according the instruction manual (Stratagene, La Jolla, CA). All mutations were validated by sequencing, and the Hice1 cDNAs were subcloned into the pQCXIP retroviral vector (Clontech).

Cell Culture and RNAi—The human osteosarcoma cell line U2OS and a virus packaging cell line, GP2-293, were cultured in DMEM supplemented with 10% FBS at 37 °C under 10% CO_2. Hice1 siRNA (Dharmacon, Lafayette, CO) was custom-synthesized according to previously validated sequences (20). siRNA was transfected into cells with Lipofectamine 2000 according to the manufacturer's instructions (Invitrogen).

Retroviral Production—Retroviral Hice1 constructs and a plasmid expressing G glycoprotein of the vesicular stomatitis virus (Clontech) were cotransfected into the GP2-293 virus packaging cell line. Virus used for infection was harvested 48 h post-transfection.

Immunofluorescence and Microscopy—U2OS cells were grown in glass-bottom dishes or on coverslips and infected with the Hice1 retrovirus using 8 μg/ml polybrene at 50% confluency. Images were captured with a Carl Zeiss Axioplan 2 microscope or an LSM710 confocal microscope. Deconvolution was performed with the Carl Zeiss Autodeblur/Autovisualize software, and the resultant maximum projections of the Z-stack images were shown.

Protein Expression and Purification—Wild-type and mutant Hice1 cDNA was cloned into the pQE31 vector (Qiagen, Hilden, Germany), and the resultant His_3-tagged Hice1 proteins were expressed in the Rosetta bacterial strain. Protein expression was induced with 0.4 mM final concentration of isopropyl 1-thio-β-D-galactopyranoside. Protein purification was performed under native conditions using protocols described in the QIAexpressionist manual (Qiagen).

In Vitro Kinase Assay—Each kinase reaction was performed using purified His-Hice1 of various concentrations and 0.4 μg of active His-Aurora-A (Upstate Biotechnology, Inc., Lake Placid, NY). Kinase and substrate were incubated at room temperature for 30 min with 100 mM of ATP, and 50 μCi [γ^{32}]ATP in 25 mM HEPES (pH 7.3), 3 mM $MgCl_2$, 3 mM MnCl2, and 25 mM β-glycerol phosphate (pH 7.3 final). Reactions were stopped by boiling samples in SDS sample buffer.

Phosphatase Treatment—U2OS cells grown in a 10-cm dishes were enriched in mitotic phase with nocodazole (200 ng/ml) for 12 h and collected by shakeoff. Cells were lysed using radioimmune precipitation assay lysis buffer (50 mM Tris-HCl (pH 7.5), 150 mM NaCl, 10 mM EDTA, 1% Nonidet P-40, 0.1% SDS, and 0.5% sodium deoxycholate). 80 μl of total cell lysate was incubated with 500 units of λPPase (New England Biolabs, Beverly, MA) with 1× phosphatase buffer and supplemented with 2 mM MnCl final. The reaction was incubated at 30 °C for 30 min.

Microtubule Cosedimentation Assay—The assay was performed according to instructions supplied by the microtubules spindown assay kit (Cytoskeleton, Inc., Denver, CO). Briefly, microtubules were assembled by incubating purified α/β-tubulin dimer proteins with 5% glycerol and 1 mM GTP in BRB80 buffer (80 mM PIPES (pH 7.0), 1 mM EGTA, 1 mM $MgCl_2$) at 35 °C for 20 min and later stabilized with 20 μM taxol. Prior to the assay, purified Hice1 protein was preclarified by ultracentrifugation in a Beckman Coulter SW 50.1 rotor at 100,000 × *g* for 40 min at 4 °C to remove potential protein aggregates. Hice1 protein was then incubated with preassembled microtubules at room temperature for 20 min and then placed on a cushion buffer (50% glycerol, 1× BRB80, and 20 μM taxol) for ultracentrifugation at 100,000 × *g* in room temperature for 20 min to pellet the Hice1-microtubule complex.

Antibody Production—A custom-synthesized peptide containing phosphorylation at serine 19 and serine 20 and a nonphospho peptide were generated and coupled with keyhole limpet hemocyanin. Peptides were used as antigens for rabbit antibody production. For the production of anti-Fam29a and anti-Ccdc5 antibodies, purified GST-fusion proteins were used as antigen for immunization in rabbits for polyclonal antibody production (GeneTex, Inc., Irvine, CA). For anti-Cep27 antibody, His_6-Cep27 was expressed, purified, and immunized into rabbits for polyclonal antibody production (GeneTex, Inc., Irvine, CA).

RESULTS

Aurora-A Binds to and Phosphorylates Hice1—To explore whether Hice1 is regulated by posttranslational modification during mitosis, we examined the electrophoretic mobility of Hice1 protein during both mitosis and interphase. U2OS cells were first enriched at mitosis by nocodazole-induced mitotic arrest and then released into drug-free media. Cell lysates were collected at various time points upon release from nocodazole treatment. Using Western blot analysis, we found that a portion of Hice1 from all mitotic stages migrated more slowly in SDS-PAGE than those from interphase (Fig. 1*A*). This decreased electrophoretic mobility was abolished when the cell lysate was treated with λ protein phosphatase (λ-PPase) (Fig. 1*B*). Together, these results suggest that Hice1 is posttranslationally modified by phosphorylation during mitosis.

We next sought to identify a regulatory kinase that may phosphorylate Hice1 during mitosis. Aurora-A is a prominent regulatory kinase involved in spindle assembly (24–28). We have previously observed that Aurora-A colocalizes with Hice1 dur-

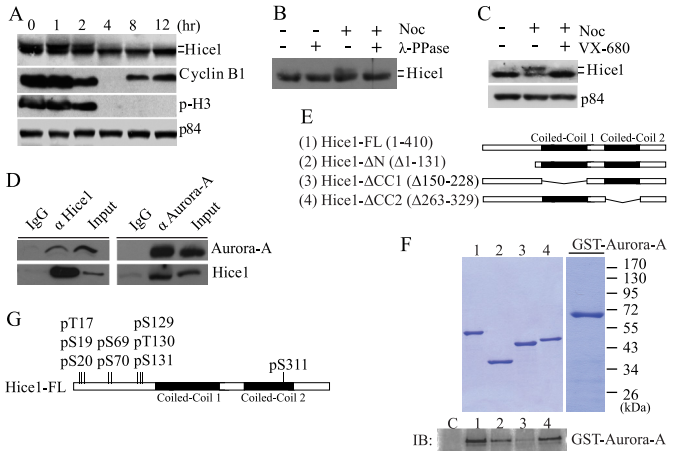

FIGURE 1. **Aurora-A binds to and phosphorylates Hice1.** *A*, Western blot analysis of Hice1 protein using U2OS cell lysate harvested at various time points after mitotic arrest with nocodazole treatment (200 ng/ml for 12 h). Phospho-histone 3 (*p-H3*) serine 10 and cyclin B1 served as makers for mitosis, whereas nuclear matrix protein p84 acted as a loading control. *B*, Western blot analysis of Hice1 protein level upon λ-PPase treatment in control and nocodazole-treated (*Noc*) U2OS cells. *C*, Hice1 protein in mock-treated (dimethyl sulfoxide) or VX-680 treated (30 μM VX-680 and 20 μM MG132, 4 h) in U2OS cells. *D*, reciprocal coimmunoprecipitation of endogenous Hice1 and Aurora-A with U2OS cell lysate. Rabbit immunoglobulin G (*IgG*) served as an immunoprecipitation control. *E*, diagram of full-length (*FL*) Hice1 and deletion constructs. *F*, *top panel*, Coomassie blue stain showing protein input level in *in vitro* binding assay between GST-Aurora-A and His-tagged Hice1-FL or Hice1 deletion mutants (*lanes 1-4*). *Bottom panel*, Western blot analysis (*IB*) on *in vitro* binding activity between GST-Aurora-A and His-Hice1. His-Hice1 proteins were incubated with immobilized metal affinity chromatography nickel-charged beads and served as baits, whereas GST-Aurora-A acted as the prey for the binding assay. *G*, summary of residues on Hice1 identified by LC/MS analysis to be phosphorylated by Aurora-A in the *in vitro* kinase assay.

ing mitosis (20). To test whether Aurora-A phosphorylates Hice1, we utilized a potent and selective Aurora-A inhibitor, VX-680 (29), to treat cells enriched in mitotic phase by nocodazole. Upon inhibition of Aurora-A by VX-680, mitosis-specific Hice1 phosphorylation was abolished, indicated by the loss of Hice1 with decreased electrophoretic mobility (Fig. 1*C*). Furthermore, Hice1 was found to associate with Aurora-A in a coimmunoprecipitation assay using endogenous proteins (Fig. 1*D*). Thus, Hice1 phosphorylation during mitosis is dependent on Aurora-A.

We then asked whether Hice1 is directly targeted by Aurora-A. We performed an *in vitro* interaction assay using purified GST-tagged Aurora-A, His-tagged Hice1, and a series of Hice1 deletion mutants. We found that the coiled-coil domain 1 (amino acids 150–228) of Hice1 is required for optimal interaction with Aurora-A (Fig. 1, *E* and *F*). Second, we sought to identify potential Aurora-A phosphorylated residues on Hice1. We performed an *in vitro* kinase assay using purified Aurora-A and His-tagged Hice1, followed by mass spectrometry on kinase reaction products. We found that Hice1 was phosphorylated by Aurora-A on multiple serine and threonine residues *in vitro*. Remarkably, with the exception of serine 311, all residues identified by the *in vitro* kinase assay reside in the N-terminal microtubule binding region as three clusters (Ser/Thr-17–20, Ser-69–70, and Ser/Thr-129–131) (Fig. 1*G*).

Identification of N-terminal S/T Clusters Important for Bipolar Spindle Formation—To determine whether these Hice1 serine and threonine clusters targeted by Aurora-A *in vitro* are important for spindle assembly *in vivo*, we screened a panel of phospho-deficient Hice1 mutants expressed in U2OS cells using spindle polarity as a functional measure. These mutants were engineered to substitute alanine for all Aurora-A targeted residues on the three Ser/Thr clusters at the N-terminal region and serine 311 at the C-terminal region (Fig. 2*A*). Additionally, all constructs were modified to harbor silent mutations that render Hice1 resistant to Hice1-specific siRNA. For the Ser/Thr-17–20 cluster, the adjacent serine 21 was also mutated to alanine to prevent compensatory phosphorylation. The resultant mutant (named 17–21A) was expressed as a C-terminally GFP-tagged protein in U2OS cells via retroviral infection, as were other mutants (69–70A, 129–131A, and S311A), respectively. All four mutants were expressed at a level similar as wild-type Hice1 (Fig. 2*B*). Although the expression levels of exogenously expressed Hice1-GFP were higher than that of endogenous Hice1, it has been shown previously that stable expression of wild-type Hice1 at this level still allows long-term cell proliferation without evident cytotoxicity (20). Because expression of GFP alone had no noticeable effect on spindle polarity compared with U2OS parental cells and the expression of Hice1 and phospho-mutants in cells depleted with endogenous Hice1 can effectively rescue cells from a previously reported Hice1 knockdown phenotype with elevated levels of multipolar cells (data not shown), we used wild-type Hice1-GFP as a control to profile the effect of mutant expression on spindle polarity. By expressing Hice1-GFP in cells simultaneously depleted with endogenous Hice1, we found that all four mutants were able to localize to the spindle and the spindle pole similarly to the wild-type (Fig. 2*C*). However, despite positive localization to mitotic spindles, two of these mutants (17–21A and 129–131A) elicited a monopolar configuration at rates significantly higher than that of the wild-type control (3-fold and 2-fold increases, respectively) (Fig. 2*D*). Meanwhile, spindles with multiple poles or less distinct configurations (*e.g.* satellite minispindles) were not detected at significantly different rates between mutants and the wild-type control (Fig. 2*D*).

Because the 17–21A mutations caused the most severe monopolar phenotype, we further examined which serine/threonine residue(s) within the Ser/Thr-17–21 cluster may account for this phenotype. Upon expression at a level similar to wild-type Hice1 (Fig. 2*E*), none of the point mutations (S17A, S19A, S20A, and S21A) or the double mutation S19–20A triggered as high a rate of monopolarity as did the 17–21A mutant (Fig. 2*F*). Taken together, these results suggest that the entire Ser/Thr-17–21 cluster, and not a single residue, is critical for early mitotic pole separation and subsequent bipolar spindle formation.

Serine 19/20 Is Phosphorylated in Vivo During Mitotic Division—The importance of the Ser/Thr-17–20 cluster in bipolar spindle formation prompted us to test whether it is an authentic Aurora-A phosphorylation site *in vivo*. We generated a phospho-specific polyclonal antibody (anti-pS19/20) that would indiscriminately recognize Hice1 phosphorylated at serine 19 and/or serine 20 (*S19/20*) (Fig. 3*A*). Using Western blot analysis, we found that the affinity-purified anti-pS19/20 antibody specifically recognized ectopically expressed wild-type Hice1 but not the phospho-deficient 17–21A mutant (Fig. 3*B*).

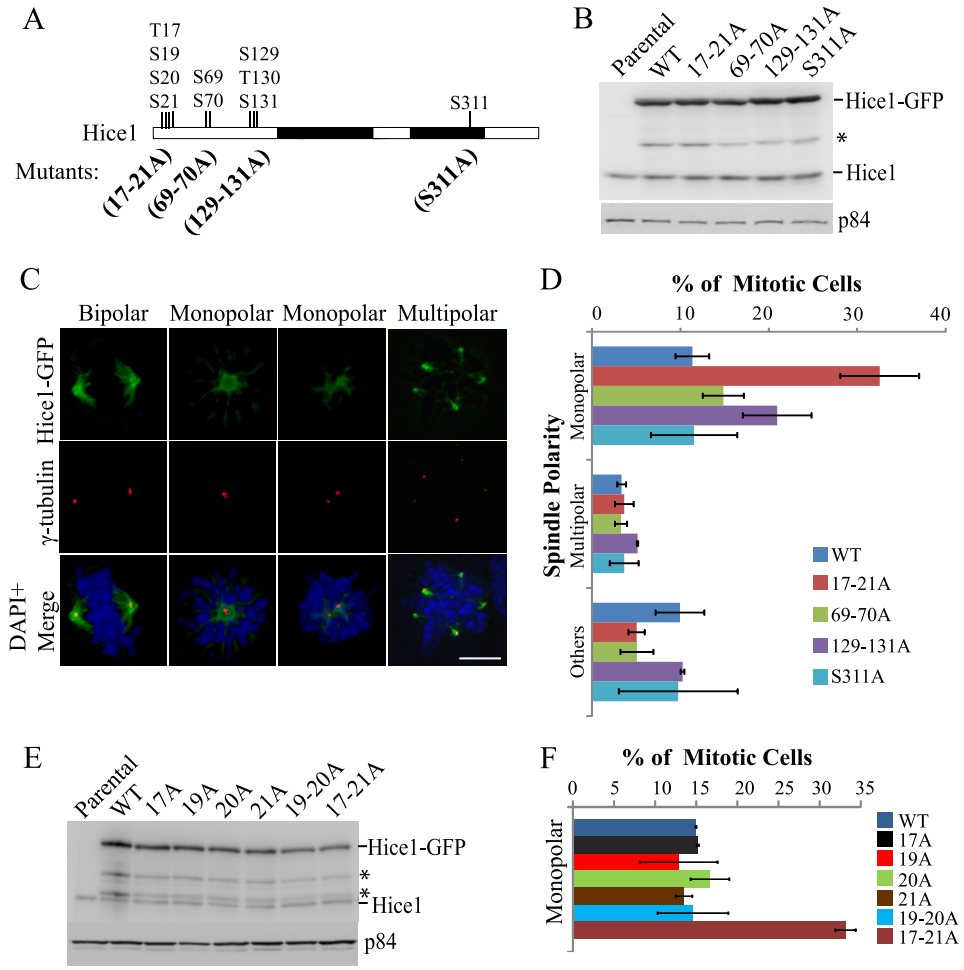

FIGURE 2. **Ser/Thr-17–21 cluster is critical for bipolar spindle formation.** *A*, illustration of the four phospho-deficient mutants. *B*, Western blot analysis with expression of GFP-tagged wild-type Hice1 and cluster or point serine/threonine-to-alanine mutants in U2OS at 48 h post-retroviral gene transfer. The *asterisk* denotes a protein degradation product. *C*, representative images of spindle morphology observed in U2OS cells expressing wild-type and phospho-deficient mutants. *Scale bar* = 5 μm. *D*, distribution of spindle morphology upon expression of Hice1-WT-GFP and phospho-deficient mutants in U2OS cells depleted of endogenous Hice1 by RNAi at 48 h post-retroviral gene transfer. Data indicate percentages from independent experiments ± S.E. $n = > 200$ per cell type. *E*, Western blot analysis showing expression of GFP-tagged Hice1 with a point or double mutation within Ser/Thr-17–21 in U2OS at 48 h post-retroviral gene transfer. The *asterisks* denote protein degradation products. *F*, distribution of spindle morphology in cells expressing wild-type, point, double, and cluster serine-to-alanine mutations within the Ser/Thr-17–21 cluster in U2OS cells depleted of endogenous Hice1 at 48 h post-retroviral gene transfer. Data indicate percentages from three independent experiments ± S.E. $n = > 150$ per cell type.

Using this antibody, we found that phosphorylation on Ser-19/20 indeed occurred on endogenous Hice1 in mitotic U2OS cells enriched by nocodazole treatment and that this phosphorylation was abolished when the cell lysate was treated with λ-PPase (Fig. 3*C*).

Next, we asked whether the pS19/20 signal could be detected at the spindle and the spindle poles. Coimmunostaining of anti-pS19/20 and anti-γ-tubulin antibodies revealed that the pS19/20 signal was primarily enriched on the spindle pole during early mitosis. However, unlike the endogenous Hice1, it was absent from the spindle proximal to the poles (Fig. 3*D*). Importantly, upon treatment of cells with either Hice1 siRNA or Aurora-A inhibitor VX-680, the pS19/20 signal was diminished on the spindle poles (Fig. 3, *E* and *F*), indicating that the observed pS19/20 signal was part of endogenous Hice1 and was dependent on Aurora-A kinase activity. Interestingly, the pS19/20 immunostaining signal at the spindle poles diminished upon anaphase entry (Fig. 3*D*) and was barely detectable on interphase centrosomes and microtubules (data not shown). These observations are consistent with earlier result showing mitosis-specific phosphorylation of Hice1 (Fig. 1*A*). Taken together, the results indicate that phosphorylation of Ser-19/20 occurs primarily in mitotic cells in an Aurora-A dependent manner and that this phosphorylation is enriched at the spindle poles.

Phosphorylation at the Ser/Thr-17–21 Cluster Inhibits Hice1 Microtubule Binding Activity—The Ser/Thr-17–21 cluster is located within the highly basic (pI = 10.04) N-terminal microtubule binding region of Hice1 (20). We speculated that phosphorylation in this region may introduce negative charges to reduce the electrostatic affinity of Hice1 toward the acidic β-tubulin tail. We therefore tested whether phosphorylation on the Ser/Thr-17–20 cluster decreases the microtubule binding activity of Hice1 *in vitro* and impairs the association of Hice1 with microtubules *in vivo*. His-tagged wild-type Hice1, the 17–21A mutant, and the 17–21E mutant (all Ser/Thr-mutated to glutamate to mimic constitutive phosphorylation) were expressed and purified to near homogeneity (Fig. 4*A*). Using

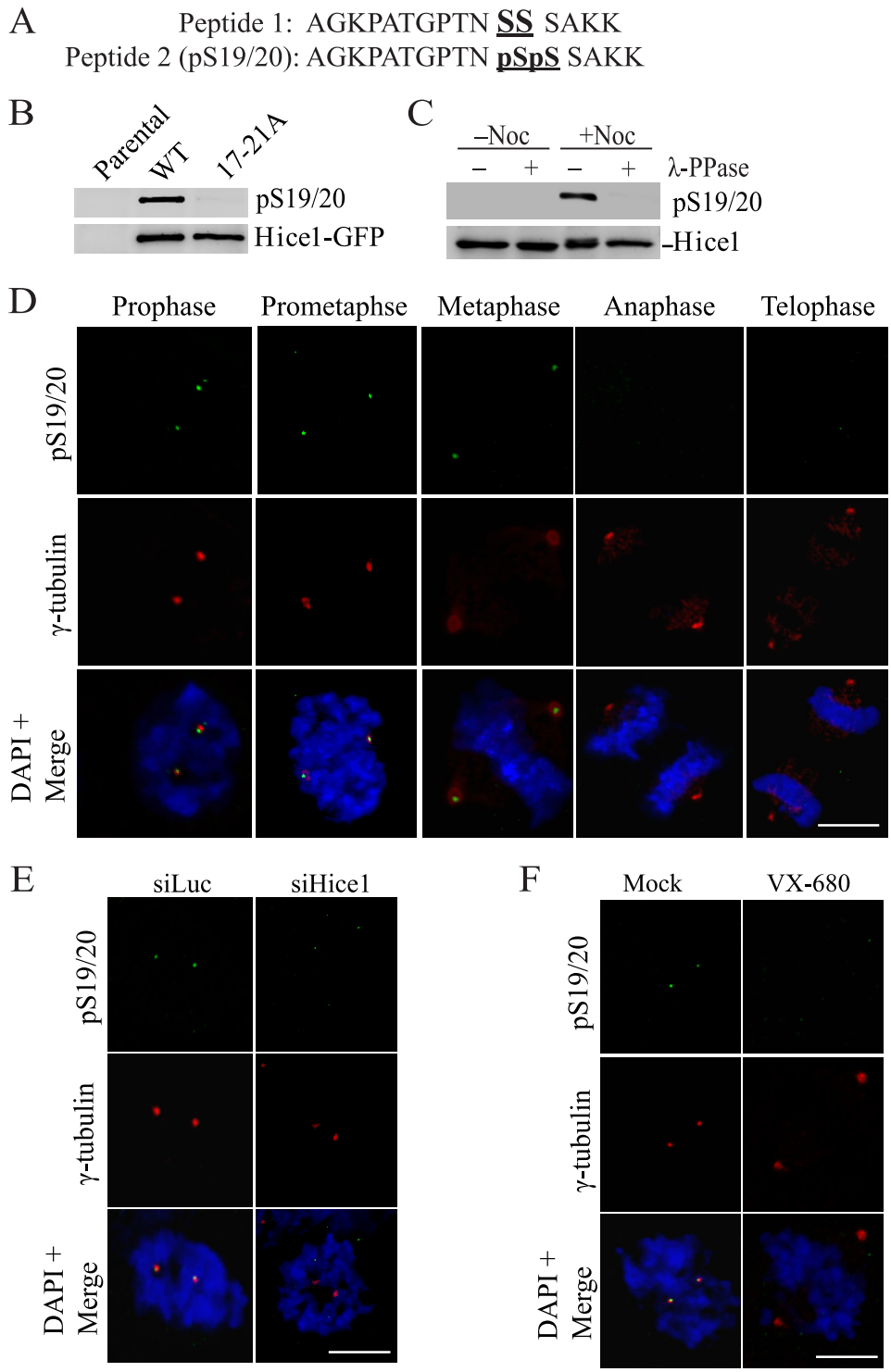

FIGURE 3. **Ser-19/20 is phosphorylated *in vivo* in an Aurora-A-dependent manner during mitotic division.** *A*, sequences of non-phosphopeptide (*Peptide 1*) and phosphopeptide (*Peptide 2*) used for the production of phospho-antibody against serine 19 and 20 (*pS19/20*). *B*, Western blot analysis utilizing pS19/20 antibody to detect exogenously expressed wild-type and 17–21A Hice1-GFP protein (*upper panel*). The membrane was stripped and reprobed with Hice1 antibody to detect the total Hice1 level (*lower panel*). *C*, Western blot analysis using pS19/20 antibody to detect phosphorylated Ser-19/20 in U2OS cells treated with or without λ-PPase. *Noc*, nocodazole. *D*, coimmunostaining of pS19/20 with γ-tubulin in cells at different stages of mitosis. *E*, coimmunostaining of pS19/20 with centrosome marker γ-tubulin in control siRNA-treated (*siLuc*) and Hice1 siRNA-treated (*siHice1*) mitotic U2OS cells. *F*, coimmunostaining of pS19/20 with γ-tubulin in mock-treated (dimethyl sulfoxide) and VX-680-treated mitotic U2OS cells (30 μM VX-680 and 20 μM MG132, 4 h). The DAPI stain shows the chromosomes. *Scale bars* = 5 μm.

microtubule cosedimentation assays, we compared the Hice1 microtubule binding activity among these three proteins. The 17–21A mutant exhibited a similar microtubule binding activity as the wild-type. Both showed moderate affinity. In contrast, the 17–21E mutant exhibited a drastically decreased binding activity (Fig. 4, *B* and *C*).

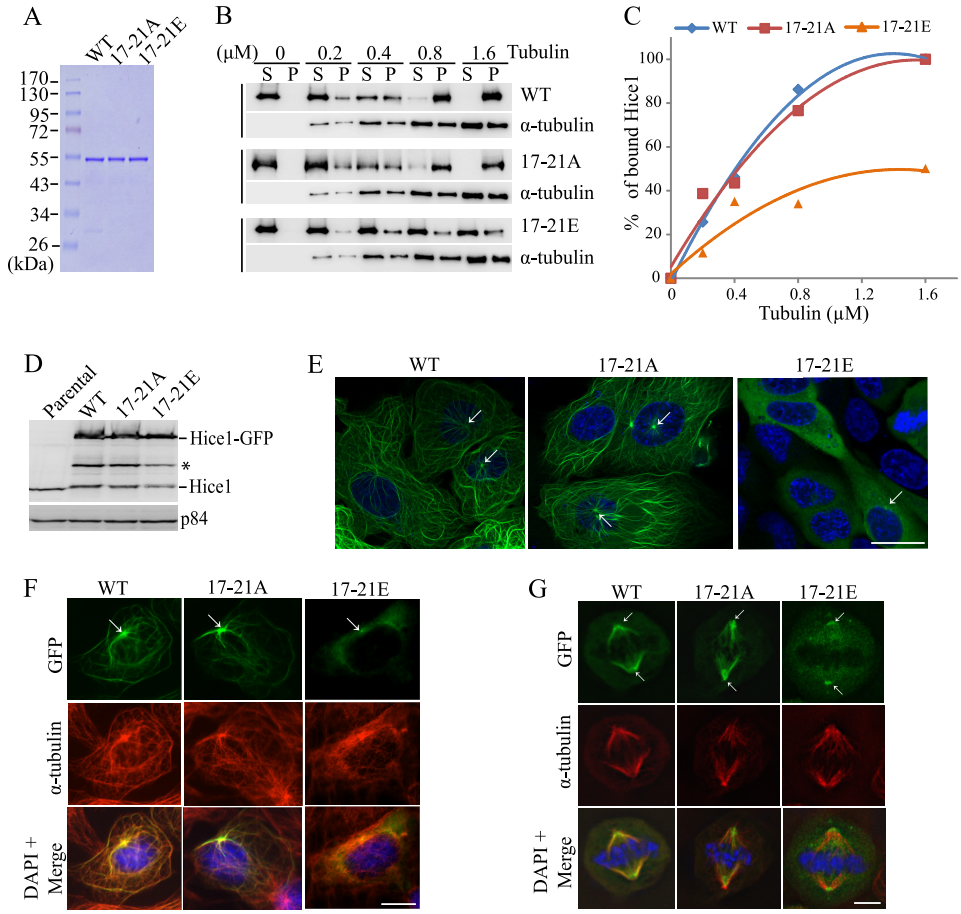

FIGURE 4. **Phosphorylation at Ser/Thr-17–21 inhibits Hice1 microtubule binding activity.** *A*, purification of His-tagged Hice1-WT, 17–21A, and 17–21E protein from Rosetta *Escherichia coli*. *B*, microtubule cosedimentation assay with Hice1. Each lane on the Western blot represents supernatant (*S*) or pellet (*P*) from cosedimentation reactions. *C*, hyperbolic plot representing Hice1 microtubule binding activity in the cosedimentation assay. Protein levels were analyzed using ImageJ software. *D*, expression of WT, 17–21A, and 17–21E Hice1-GFP protein in U2OS cells at 48 h post-retroviral infection. The *asterisk* denotes protein degradation products. *E*, live-cell images of U2OS cells expressing Hice1-GFP. *Scale bar* = 10 μm. *F* and *G*, coimmunostaining of Hice1-GFP with α-tubulin in interphase and mitotic U2OS cells. The *arrows* in *E*, *F*, and *G* indicate centrosomes. *Scale bars* = 5 μm.

To determine whether the decrease in microtubule binding activity also occurs *in vivo*, the 17–21E mutant was expressed in U2OS cells via retroviral infection. The 17–21E mutant was readily expressed at a level similar to that of wild-type Hice1 and the 17–21A mutant (Fig. 4*D*). The 17–21E mutant localized only to spindle poles and was absent from interphase microtubule asters (Fig. 4, *E* and *F*) and mitotic spindles (*G*). Taken together, these results suggest that phosphorylation on the Ser/Thr-17–21 cluster may negatively regulate Hice1 microtubule binding activity *in vitro* and *in vivo*.

Phospho-mimic Mutation at Ser/Thr-17–21 Reduces Intraspindle Microtubule Nucleation—Next we sought to understand the functional consequence of phosphorylation of the Ser/Thr-17–21. Hice1 is known to contribute to spindle assembly in part by playing a critical role in intraspindle microtubule nucleation. Because phosphorylation inhibits Hice1 localization to the spindle, we then examined whether phosphorylation affects intraspindle microtubule nucleation. By expressing mutant Hice1 in U2OS cells depleted of endogenous Hice1, we found that expression of the 17–21E mutant significantly reduced intraspindle microtubule intensity by 40% compared with the wild-type control. Expression of the 17–21A mutant, on the other hand, did not significantly alter the intraspindle microtubule intensity (Fig. 5, *A* and *B*).

Phospho-mimic Mutation Does Not Affect Augmin Complex Formation but Hampers Localization of Augmin Components to the Spindle—Among all the currently known components of the Augmin complex, only Hice1 has been demonstrated to have a direct microtubule binding activity *in vitro*. Because phospho-mimic mutation hampers Hice1 localization and, consequently, intraspindle nucleation, we explored the effect of phosphorylation on Augmin complex formation and localization. Immunoprecipitation of Hice1 from cells expressing wild-type, 17–21A, and 17–21E (endogenous Hice1 simultaneously depleted) revealed that all three proteins can associate with Augmin components Fam29a, Cep17, and Ccdc5 in the cell (Fig. 5*C*), suggesting that phosphorylation does not affect Augmin complex formation. Utilizing an antibody useful in immunostaining (anti-Fam29a), we found that expression of 17–21E led to a reduced level of Fam29a intensity in the spindle in cells depleted of endogenous Hice1 (Fig. 5, *D* and *E*), suggesting that the microtubule binding activity of Hice1 may affect Augmin complex function.

Phosphorylation at Ser/Thr-17–21 Mediates Proper Spindle Assembly for Efficient and Accurate Mitotic Cell Division—To determine how phosphorylation affects cell cycle progression

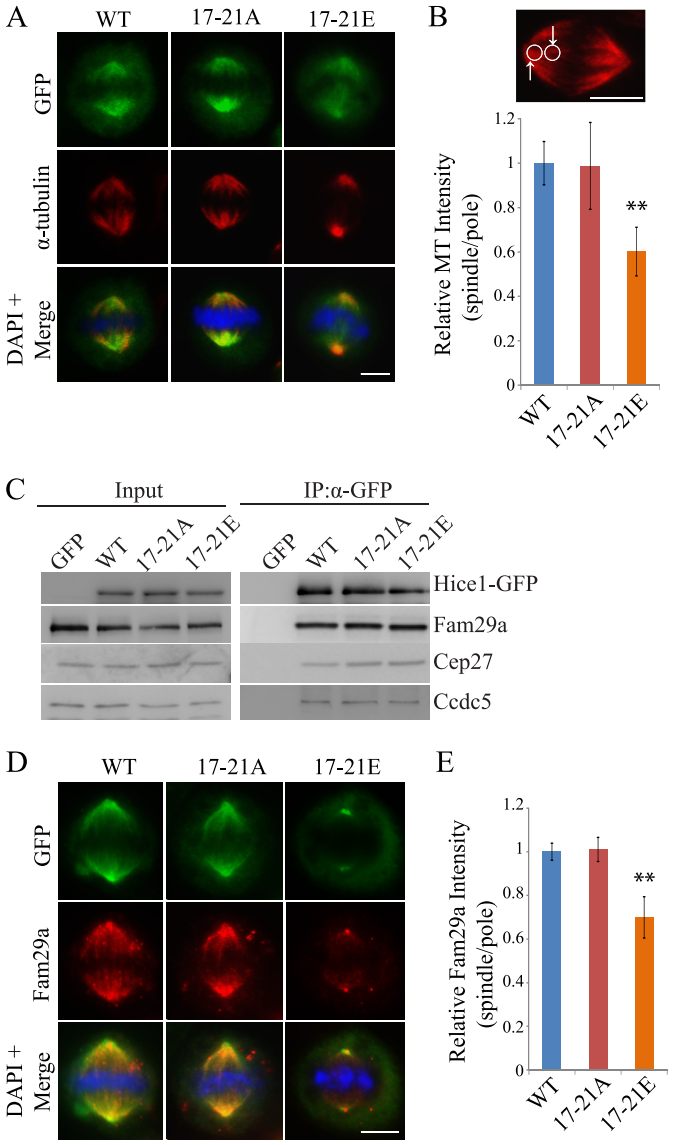

FIGURE 5. **Hice1 phospho-mimic mutation reduces intra-spindle microtubule nucleation.** *A* and *B*, representative images and quantitation of relative α-tubulin intensity (*spindle/pole*) were shown in U2OS cells expressing Hice1-GFP with endogenous Hice1 depleted by RNAi. Quantitation was performed with ImageJ software on maximum image projection. Data show relative mean spindle/pole α-tubulin intensity ± S.E. $n = 15$ per cell type; **, $p <$ 0.001). *C*, coimmunoprecipitation (*IP*) of Hice1-GFP with three representative proteins of the Augmin complex (Fam29a, Cep27, and Ccdc5). *D* and *E*, representative images and quantitation of relative Fam29a intensity (*spindle/pole*) in U2OS expressing GFP with control siRNA treatment or Hice1-GFP with endogenous Hice1 depleted by RNAi. Quantitation was performed with ImageJ software on maximum image projection. Data show relative mean spindle/pole Fam29a intensity ± S.E. $n = 14$ per cell type; **, $p < 0.0001$. The DAPI stain shows the chromosomes. *Scale bars* = 5 μm.

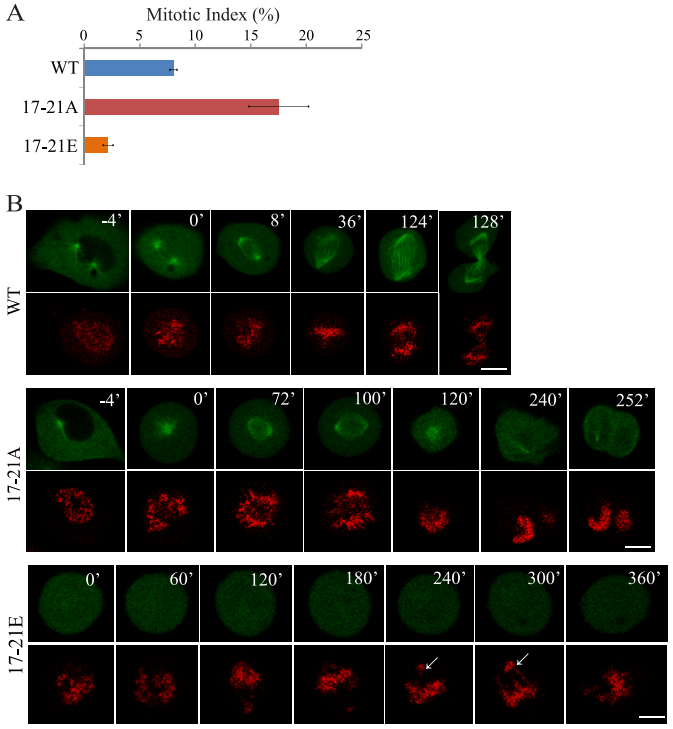

FIGURE 6. **Phospho-mutation at Ser/Thr-17–21 impairs efficient mitotic progression.** *A*, the mitotic index of U2OS cells 48 h post-retroviral infection with Hice1 retroviruses, whereas endogenous Hice1 was depleted by siHice1. Data show the mean mitotic index from three independent experiments ± S.E. $n = > 1200$. *B*, time-lapse microscopy of U2OS cells coexpressing H2B-mcherry and Hice1-GFP 48–55 h post-retroviral infection. Hice1 RNAi was used to simultaneously deplete the endogenous protein. The *arrows* indicate misaligned metaphase chromosomes. *Scale bars* = 5 μm.

and mitotic cell division, we examined the mitotic index and mitotic progression in cells expressing Hice1-GFP in cells depleted of endogenous Hice1. Results revealed that phospho-mutation hampers efficient mitotic progression and bipolar spindle formation (Fig. 6, *A* and *B*). Expression of 17–21A led to an elevated level of the mitotic index when compared with the wild-type control (Fig. 6*A*). Time-lapse analysis showed that wild-type cells' mitotic progression from nuclear envelop breakdown to anaphase onset took an average of ~77 min ($n =$ 18). On the other hand, 17–21A cells exhibited severe defects in bipolar spindle assembly and mitotic progression, with 47.3% of cells (36 of 76) remaining in a monopolar state during the entire time-lapse experiment (7 h). Furthermore, 23.7% (18 of 76) of 17–21A cells underwent mitotic catastrophe. Additionally, 30% of 17–21A cells (22 of 76) had delayed progression and took an average of ~198 min to progress through mitosis. They showed erratic spindle configuration changes during the course of mitotic progression, including the collapse of the bipolar spindle into a monopolar spindle and often exited mitosis without undergoing cytokinesis (Fig. 6*B*). The expression of 17–21E cells led to a low level of the mitotic index (2%) compared with the wild-type control (8%) (Fig. 6*A*). Time-lapse analysis showed that 17–21E cells were also unable to undergo efficient mitotic progression, with 7 of 12 cells arrested in mitosis (> 7 h) with a poorly aligned metaphase plate and lagging chromosomes (Fig. 6*B*). Altogether, these results suggest that timely phosphorylation and dephosphorylation of Hice1 at Ser/Thr-17–21 are both important for mitotic progression and the establishment of a stable bipolar spindle.

The ultimate purpose of proper spindle assembly is to ensure chromosome alignment and accurate segregation into progeny cells. Because we observed a defect in cytokinesis and poorly aligned metaphase chromosomes in time-lapse experiments, we proceeded to evaluate the rate of chromosome misalignment and micronuclei and multinuclei formation. We found that in either mutant, the rates of chromosome misalignment were significantly higher than in the wild-type control (Fig. 7, *A* and *B*). Conse-

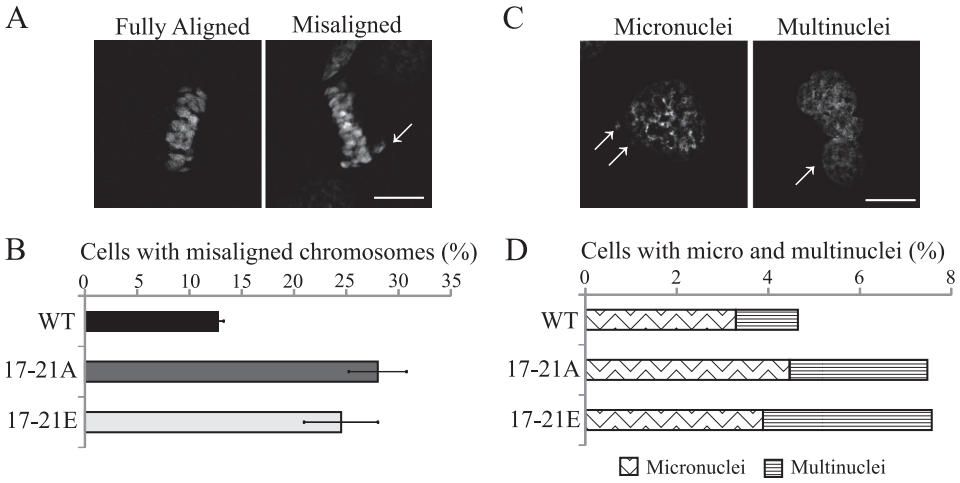

FIGURE 7. **Phospho-mutation at Ser/Thr-17–21 triggers elevated levels of chromosome misalignment and segregation errors.** *A* and *B*, representative images and quantitation of the percentage of misaligned chromosomes in U2OS cells expressing GFP or Hice1-GFP at 48 h post-retroviral infection. Hice1 RNAi was used to simultaneously deplete the endogenous protein. The *arrows* indicate misaligned metaphase chromosomes. Data indicate mean percentages from three independent experiments ± S.E. $n = > 100$ per cell type). *C* and *D*, representative images and quantitation of the percentage of micro- or multi-nucleated U2OS cells expressing GFP or Hice1-GFP at 96 h post-retroviral infection while endogenous Hice1 was simultaneously depleted by RNAi. The *arrows* indicate micronuclei (*C*, *left panel*) and multinuclei (*right panel*). Data indicate percentages from three independent experiments. $n = > 1000$ per cell type). *Scale bars* = 5 μm.

quently, these two mutants caused a greater rate of formation of cells with micronuclei and multinuclei (Fig. 7, *C* and *D*) than the wild-type control, suggesting that proper phosphorylation of Hice1 during mitosis is critical for accurate chromosome segregation.

DISCUSSION

Hice1 is a microtubule binding protein important for mitotic spindle assembly and chromosome segregation. This study demonstrates that the microtubule binding domain of Hice1 is phosphorylated on multiple serine/threonine clusters by the mitotic kinase Aurora-A. In particular, phosphorylation of one of the serine/threonine clusters, Ser/Thr-17–21, negatively regulates the microtubule binding activity of Hice1. This phosphorylation of Hice1 occurs primarily during mitosis and is critical for pole separation and subsequent formation of a dynamic and stable bipolar spindle.

The observed mitotic phosphorylation of Hice1 requires the kinase activity of Aurora-A. First, Hice1 directly interacts with Aurora-A *in vitro* and associates with Aurora-A *in vivo* (Figs. 1 and 3). Second, at least half of all Hice1 species are phosphorylated during prometaphase, which can be diminished by treating cells with a selective Aurora-A inhibitor, VX-680 (Fig. 1, *A* and *C*). In particular, the Ser/Thr-17–21 cluster can be phosphorylated *in vivo* in an Aurora-A-dependent manner. The patterns of spatial distribution and regulatory timing of Hice1 phosphorylation at Ser-19/20 match those of Aurora-A activity (Fig. 3).

Hice1 phosphorylation at the Ser/Thr-17–21 cluster was observed in mitotic cells from prophase to metaphase and begins to diminish in anaphase (Fig. 3*D*). This temporal pattern of phosphorylation is consistent with that of Aurora-A in that Hice1 phosphorylation peaks during early mitosis and falls during anaphase when it is targeted for degradation by Cdh1-APC (30–33). The loss of phosphorylated Ser/Thr-17–21 in late mitosis may be regulated in a similar manner because we also observed a down-regulation of Hice1 during late mitosis (Fig. 1*A*). Alternatively, Ser/Thr-17–21 may be targeted by mitotic phosphatases. Protein phosphatase 1 has been implicated to function in a feedback loop counterbalancing Aurora kinase activity (34, 35). Therefore, it may play a role in regulating the phosphorylation status of Hice1 at Ser/Thr-17–21.

Phosphorylation on the Ser/Thr-17–21 cluster significantly reduces the microtubule binding activity of Hice1, likely by altering the surface charge of the protein. The Ser/Thr-17–21 cluster is located in the microtubule binding region enriched with basic residues and serine/threonine residues. This composition may allow delicate regulation of microtubule binding activity via changes of surface charge by phosphorylation. When Hice1 is not phosphorylated, the basic residues may provide electrostatic affinity for the acidic tail of β-tubulin to allow microtubule binding. Once Hice1 is phosphorylated, the basic residues would be neutralized, leading to attenuated electrostatic affinity and hence release of Hice1 from microtubules. A similar mode of regulation by Aurora-A and other mitotic kinases has been reported. Examples of phosphorylation that negatively regulate microtubule binding activity of a spindle-associated protein include the activity of MAP2, MAP4, Kif2a, DDAC, p150glued, and RASSF1A (36–40).

Phosphorylation of the Ser/Thr-17–21 cluster is important for proper separation of spindle poles in opposite directions and for stable bipolar spindle morphology. On one hand, the 17–21A phenotypes are consistent with the known role of Aurora-A in regulating pole separation and maintaining proper spindle morphology. These phenotypes suggest that Hice1 may act downstream of Aurora-A during pole separation, perhaps by coordinating with other Aurora-A substrates. On the other hand, the 17–21E mutant triggers an evident defect in intraspindle microtubule nucleation. Meanwhile, Hice1 was reported to be critical for regulating the spindle integrity during mitosis (14, 16, 20). Depletion of Hice1 by RNAi in human cells

results in predominately multipolar spindles associated with reduced spindle microtubule intensity (14, 16). These phenotypes triggered by Hice1 depletion do not conflict with those caused by 17–21 mutant expression. Instead, the partly overlapping mitotic phenotypes may stem from a common regulation of Hice1 microtubule binding that is likely to be quite delicate.

We have shown previously that Hice1 binds to and stabilizes microtubules *in vitro* and in cells when it is overexpressed (20). In mitotic cells, the microtubule binding and stabilizing activity of Hice1 is likely to be regulated in a stage-dependent manner during mitosis. During the late G_2 phase, this activity is restrained to promote faster microtubule turnover, thus allowing timely poleward movement of centrosomes by microtubule based motors such as Eg5. Overexpression of Hice1, particularly the 17–21A mutant whose microtubule binding activity cannot be restrained, may enhance the microtubule stability and decrease the microtubule dynamics, leading to delayed pole separation (that is, monopolarity). In contrast, because of reduced microtubule binding activity, the 17–21E mutation does not delay the pole separation.

During the progression toward prometaphase and metaphase, the microtubule activity of Hice1 is gradually unleashed to allow proper intraspindle microtubule formation. This is critical for establishing a bipolar spindle with adequate "strength" and functionality. Insufficient spindle microtubule intensity may destabilize established bipolar configurations. The observed aberrancy in the 17–21E mutant closely mimics that from knockdown of various Augmin components, highlighted by reduced metaphase spindle intensity (Fig. 5, *A* and *B*), chromosome misalignment (Figs. 6*B* and 7*A*), and increased multinuclei formation (Fig. 7*B*) (14, 16, 18, 20). As for the 17–21A mutant, the overall dynamics of microtubules is compromised from the beginning because of unrestrained microtubule binding. The resultant monopolar spindles, albeit dissolvable after long delay, are still inherently faulty and may undergo erratic configuration changes (Fig. 6*B*).

Within the Augmin complex, only Hice1 has been demonstrated to possess direct microtubule binding in an *in vitro* assay using purified Hice1 (20), whereas the other components may associate with the microtubule indirectly (13, 18). Thus, Hice1 serves as an anchor of the Augmin complex to bind the microtubule. Our study supports this possibility (Fig. 5, *A* and *B*). Although phosphorylation at Ser/Thr-17–21 does not affect Augmin complex formation (Fig. 5*C*), expression of 17–21E in cells leads to a decrease in Fam29a localization to the spindle (Fig. 5, *D* and *E*), suggesting that Hice1 may be critical for the binding of the Augmin complex to the spindle.

Mechanistically, phosphorylation on the Ser/Thr-17–21 cluster may serve either to prevent Hice1 from loading onto the spindle or to strip Hice1 off the spindle when it is no longer needed. This idea is supported by the distribution pattern of pS19/20, the reduced microtubule binding *in vitro*, and diminished microtubule association *in vivo* in the 17–21E mutant. Fluorescence recovery after photobleaching (FRAP) analysis done by another research group showed that Dgt5, a *Drosophila* homolog of an Augmin component, has a short half-life on the metaphase spindle ($t_{1/2} = 4$ s), suggesting that rapid association and disassociation occur *in vivo* (13). If the human Augmin complex also has a similar half-life on the metaphase spindle, then phosphorylation of Hice1 at Ser/Thr-17–21 may be critically important for rapid loading and removal of the Augmin complex on and off the spindle.

Hice1 is important for proper chromosome alignment and segregation (20). Consistent with previous reports, we have found that Hice1 phospho-mutations lead to increased rates of chromosome misalignment and segregation errors (Fig. 7). Therefore, this newly uncovered role for Aurora-A in regulating the microtubule binding activity of Hice1 is central to faithful segregation and to curbing the potential for tumorigenic aneuploidy.

Acknowledgments—We thank Dr. Guowei Fang for the Fam29a plasmid, Dr. Erica Golemis for the Ccdc5 plasmid, and Dr. Laurence Pelletier for the Cep27 plasmid and antibody. We thank Yi-Tzu Lin, whose initial observation contributed to the establishment of the project. We also thank Dr. Yumay Chen and Dr. Phang-Lang Chen for insightful discussions. We thank Guideng Li, Dr. Dennis Wang, and Dr. Randy Wei for technical assistance.

REFERENCES

1. Gadde, S., and Heald, R. (2004) *Curr. Biol.* **14,** R797–R805
2. Kline-Smith, S. L., and Walczak, C. E. (2004) *Mol. Cell* **15,** 317–327
3. O'Connell, C. B., and Khodjakov, A. L. (2007) *J. Cell Sci.* **120,** 1717–1722
4. Heald, R., and Walczak, C. E. (2009) in *The Kinetochore,* pp 1–38, Springer, New York
5. Lüders, J., and Stearns, T. (2007) *Nat. Rev. Mol. Cell Biol.* **8,** 161–167
6. Wiese, C., and Zheng, Y. (2006) *J. Cell Sci.* **119,** 4143–4153
7. Gruss, O. J., and Vernos, I. (2004) *J. Cell Biol.* **166,** 949–955
8. Heald, R., Tournebize, R., Blank, T., Sandaltzopoulos, R., Becker, P., Hyman, A., and Karsenti, E. (1996) *Nature* **382,** 420–425
9. Kaláb, P., Pralle, A., Isacoff, E. Y., Heald, R., and Weis, K. (2006) *Nature* **440,** 697–701
10. Kalab, P., and Heald, R. (2008) *J. Cell Sci.* **121,** 1577–1586
11. Kalab, P., Weis, K., and Heald, R. (2002) *Science* **295,** 2452–2456
12. Goshima, G., and Kimura, A. (2010) *Curr. Opin. Cell Biol.* **22,** 44–49
13. Goshima, G., Mayer, M., Zhang, N., Stuurman, N., and Vale, R. D. (2008) *J. Cell Biol.* **181,** 421–429
14. Lawo, S., Bashkurov, M., Mullin, M., Ferreria, M. G., Kittler, R., Habermann, B., Tagliaferro, A., Poser, I., Hutchins, J. R., Hegemann, B., Pinchev, D., Buchholz, F., Peters, J. M., Hyman, A. A., Gingras, A. C., and Pelletier, L. (2009) *Curr. Biol.* **19,** 816–826
15. Meireles, A. M., Fisher, K. H., Colombié, N., Wakefield, J. G., and Ohkura, H. (2009) *J. Cell Biol.* **184,** 777–784
16. Uehara, R., Nozawa, R. S., Tomioka, A., Petry, S., Vale, R. D., Obuse, C., and Goshima, G. (2009) *Proc. Natl. Acad. Sci. U.S.A.* **106,** 6998–7003
17. Wainman, A., Buster, D. W., Duncan, T., Metz, J., Ma, A., Sharp, D., and Wakefield, J. G. (2009) *Genes Dev.* **23,** 1876–1881
18. Zhu, H., Coppinger, J. A., Jang, C. Y., Yates, J. R., 3rd, and Fang, G. (2008) *J. Cell Biol.* **183,** 835–848
19. Zhu, H., Fang, K., and Fang, G. (2009) *Mol. Cells* **27,** 1–3
20. Wu, G., Lin, Y. T., Wei, R., Chen, Y., Shan, Z., and Lee, W. H. (2008) *Mol. Cell. Biol.* **28,** 3652–3662
21. Wu, G., Wei, R., Cheng, E., Ngo, B., and Lee, W. H. (2009) *Mol. Biol. Cell* **20,** 4686–4695
22. Marumoto, T., Zhang, D., and Saya, H. (2005) *Nat. Rev. Cancer* **5,** 42–50
23. Barr, A. R., and Gergely, F. (2007) *J. Cell Sci.* **120,** 2987–2996
24. Glover, D. M., Leibowitz, M. H., McLean, D. A., and Parry, H. (1995) *Cell* **81,** 95–105
25. Roghi, C., Giet, R., Uzbekov, R., Morin, N., Chartrain, I., Le Guellec, R., Couturier, A., Dorée, M., Philippe, M., and Prigent, C. (1998) *J. Cell Sci.*

111, 557–572
26. Hannak, E., Kirkham, M., Hyman, A. A., and Oegema, K. (2001) *J. Cell Biol.* **155,** 1109–1116
27. Liu, Q., and Ruderman, J. V. (2006) *Proc. Natl. Acad. Sci. U.S.A.* **103,** 5811–5816
28. Cowley, D. O., Rivera-Pérez, J. A., Schliekelman, M., He, Y. J., Oliver, T. G., Lu, L., O'Quinn, R., Salmon, E. D., Magnuson, T., and Van Dyke, T. (2009) *Mol. Cell. Biol.* **29,** 1059–1071
29. Harrington, E. A., Bebbington, D., Moore, J., Rasmussen, R. K., Ajose-Adeogun, A. O., Nakayama, T., Graham, J. A., Demur, C., Hercend, T., Diu-Hercend, A., Su, M., Golec, J. M., and Miller, K. M. (2004) *Nat. Med.* **10,** 262–267
30. Arlot-Bonnemains, Y., Klotzbucher, A., Giet, R., Uzbekov, R., Bihan, R., and Prigent, C. (2001) *FEBS Lett.* **508,** 149–152
31. Floyd, S., Pines, J., and Lindon, C. (2008) *Curr. Biol.* **18,** 1649–1658
32. Littlepage, L. E., and Ruderman, J. V. (2002) *Genes Dev.* **16,** 2274–2285
33. Taguchi, S., Honda, K., Sugiura, K., Yamaguchi, A., Furukawa, K., and Urano, T. (2002) *FEBS Lett.* **519,** 59–65
34. Kim, Y., Holland, A. J., Lan, W., and Cleveland, D. W. (2010) *Cell* **142,** 444–455
35. Katayama, H., Zhou, H., Li, Q., Tatsuka, M., and Sen, S. (2001) *J. Biol. Chem.* **276,** 46219–46224
36. Illenberger, S., Drewes, G., Trinczek, B., Biernat, J., Meyer, H. E., Olmsted, J. B., Mandelkow, E. M., and Mandelkow, E. (1996) *J. Biol. Chem.* **271,** 10834–10843
37. Jang, C. Y., Coppinger, J. A., Seki, A., Yates, J. R., 3rd, and Fang, G. (2009) *J. Cell Sci.* **122,** 1334–1341
38. Jang, C. Y., Coppinger, J. A., Yates, J. R., 3rd, and Fang, G. (2011) *Biochem. Biophys. Res. Commun.* **408,** 174–179
39. Romé, P., Montembault, E., Franck, N., Pascal, A., Glover, D. M., and Giet, R. g. (2010) *J. Cell Biol.* **189,** 651–659
40. Rong, R., Jiang, L. Y., Sheikh, M. S., and Huang, Y. (2007) *Oncogene* **26,** 7700–7708